

Studies on the assembly of a leucine zipper antibacterial peptide and its analogs onto mammalian cells and bacteria

Aqeel Ahmad · Sarfuddin Azmi · Jimut Kanti Ghosh

Received: 8 May 2010 / Accepted: 2 September 2010 / Published online: 21 September 2010
© Springer-Verlag 2010

Abstract Membrane-interaction and assembly of a leucine zipper peptide (LZP), and its single (SASA) and double (DASA) alanine-substituted analog onto mammalian, hRBCs and 3T3 cells and bacteria, *Escherichia coli* and *Staphylococcus aureus* were studied as a model system to understand the plausible role of assembly on their contrasting cytotoxic but similar bactericidal activities. Peptides' ability to depolarize and damage the membrane organization of hRBC and 3T3 cells decreased from LZP to SASA and to DASA which may be related to their decrease in assembly onto these mammalian live cells and oligomerization states in the presence of these cell membranes or zwitterionic PC/Chol lipid vesicles. However, LZP and its analogs showed appreciable similarities in damaging or depolarizing the *E. coli* or *S. aureus* cells, which further matched with their comparable assembly and oligomerization either onto these live cells or the cell membranes or in the presence of negatively charged PC/PG lipid vesicles.

Keywords Antimicrobial peptides, bactericidal and cytotoxic activity · Cellular interactions · Peptide-induced depolarization and damage of membrane organization of bacteria and mammalian cells · Leucine zipper motif · Assembly and oligomerization of antibacterial peptides

Abbreviations

hRBCs	Human red blood cells
Fmoc	<i>N</i> -(9-Fluorenyl) methoxycarbonyl
Chol	Cholesterol
HPLC	High performance liquid chromatography
CFU	Colony forming unit
PC	Egg phosphatidylcholine
PG	Egg phosphatidylglycerol
NBD	4-Fluoro-7-nitrobenz-2-oxa-1,3-diazole
MALDI-TOF	Matrix-assisted laser desorption ionization time-of-flight
PBS	Phosphate-buffered saline
MICs	Minimum inhibitory concentrations
MTT	3-(4,5-Dimethylthiazol-2-yl)-2,5-diphenyltetrazolium bromide
FRET	Fluorescence resonance energy transfer
LUV	Large unilamellar vesicles
FITC	Fluorescein isothiocyanate

Introduction

Antimicrobial peptides are evolutionary ancient weapons and effective components of innate immune system (Boman 1995; Zasloff 2002). Many of the antimicrobial peptides exhibit immunomodulatory properties to the host (Hancock and Sahl 2006; Lai and Gallo 2009; Yeaman and Yount 2007). Antimicrobial peptides show various modes of actions (Nicolas 2009). Some of these peptides do not cause membrane permeabilization but are still proficient to cause bacterial death. These antimicrobial peptides, which include proline/arginine-rich pyrrhocoricin, drosocin and Bac-7 (Li et al. 2006; Otvos et al. 2005; Podda et al. 2006),

The CDRI communication number of this manuscript is 7202.

Electronic supplementary material The online version of this article (doi:10.1007/s00726-010-0744-7) contains supplementary material, which is available to authorized users.

A. Ahmad · S. Azmi · J. K. Ghosh (✉)
Molecular and Structural Biology Division, Central Drug
Research Institute, CSIR, Lucknow 226001, India
e-mail: jighosh@yahoo.com

histidin-rich human antimicrobial peptide histatin-5 (Luque-Ortega et al. 2008) and pleurocidin derived antimicrobial peptide (Patrzykat et al. 2002), can translocate across the membrane and accumulate intracellularly, and target various cellular components to inhibit bacterial growth.

However, the primary target of most of the antimicrobial peptides is the bacterial membrane. These peptides kill bacteria rapidly by the physical disruption of cell membrane and leave limited scope for bacterial resistance. Therefore, there have been tremendous interests in antimicrobial peptides for the last several years (Hancock 1997; Hilpert et al. 2005; Marr et al. 2006; Zasloff 2006) in the development of new potential antibacterial drugs. Hemolytic activity of the antimicrobial peptides, which is a measure of their cytotoxic activity, has been correlated with their hydrophobicity, amphipathicity, and helicity (Chen et al. 2005). Although amphipathic nature of the peptides is essential for their biological activity, it is not clearly known, which factors actually control their bactericidal activity. Sometimes the antimicrobial activity of the peptides is less dependent on high hydrophobicity or helicity (Oren and Shai 1997). It seems that the assembly of these peptides in aqueous environment is also a key determinant of their cytotoxic and antibacterial activities (Asthana et al. 2004; Chen et al. 2005; Ghosh et al. 1997; Glukhov et al. 2005; Javadvpour and Barkley 1997; Oren et al. 1999).

Despite a number of comprehensive studies the possible role of assembly of antimicrobial peptides in a particular mammalian cell or bacteria in determining their cytotoxic and antibacterial activity against the respective cell is poorly understood. Recently, an amphipathic leucine zipper peptide (LZP) and several of its analogs in which leucine residue (s) at 'a' and/or 'd' position (s), substituted by alanine residue (s) have been designed and

characterized (Ahmad et al. 2006). Interestingly, although the substitution of leucine residues significantly and progressively reduced the lytic activity of the LZP against human red blood cells (hRBCs), it had almost negligible effects on the antibacterial activity of LZP. Electron microscopic studies showed a similar total lysis with change of morphology of *Escherichia coli* cells in the presence of either LZP or its alanine substituted analogs (Ahmad et al. 2006). However, it was not known how these peptides bind and assemble onto hRBCs and bacteria. The present work has been aimed to study membrane-interaction and assembly of the LZP, a single alanine-substituted analog (SASA) and a double alanine-substituted analog (DASA) onto two mammalian cells, namely hRBCs and murine 3T3, and two strains of *E. coli*, namely *E. coli* DH5 α (*E. coli*) and *E. coli* ATCC 10536, and *Staphylococcus aureus* ATCC 9144 (*S. aureus*) to understand how cellular assembly of these peptides influence on their cytotoxic and antibacterial activity against a particular cell (Table 1).

Materials and methods

Materials

Rink amide MBHA resin (loading capacity, 0.63 mmol/g) and all the N- α Fmoc and side-chain protected amino acids were purchased from Novabiochem, Laufelfingen, Switzerland. Coupling and other reagents for solid phase peptide syntheses and cleavage of peptides from the resin as reported before (Ahmad et al. 2006; Asthana et al. 2004; Yadav et al. 2003) were either purchased from Sigma, New Delhi, India or from reputed local companies. Acetonitrile (HPLC grade) was procured from Merck, Mumbai, India while trifluoroacetic acid (TFA) was purchased from

Table 1 Amino acid sequences of the designed leucine zipper peptides

Peptide designation	Amino acid sequences (X=H or NBD or Rhodamine) (Amino acids at 'a' and 'd' positions are bold and substituted amino acids are bold, italic and underlined)
	a b c d e f g a b c d e f g a b c d e f g
LZP	X-NH-L K A L K K A L K W L K K A L K A L K K A-CONH ₂
SASA [LZP (L8A)]	X-NH-L K A L K K A <u>A</u> K W L K K A L K A L K K A-CONH ₂
DASA [LZP (L8A/L11A)]	X-NH-L K A L K K A <u>A</u> K W <u>A</u> K K A L K A L K K A-CONH ₂

Sigma, New Delhi, India. Egg phosphatidylcholine (PC), egg phosphatidylglycerol (PG) were procured from Northern Lipids Inc., Burnaby BC V5J5J1, Canada while cholesterol (Chol) was purchased from Sigma, New Delhi, India. Tetramethylrhodamine succinimidyl ester (Rho) and NBD (4-fluoro-7-nitrobenz-2-oxa-1, 3-diazole) -fluoride were purchased from Molecular Probes (Eugene, OR). Rest of the reagents were of analytical grade and procured locally; buffers were prepared in milli Q water (USF^{ELGA}).

Cell cultures

3T3 mouse fibroblast cell lines were grown in DMEM supplemented with 10% fetal calf serum and antibiotics, at 37°C in a humidified atmosphere at 5% CO₂ and 95% air. Cells were counted with the help of a LEICA DM 5000 Microscope, Leica Microsystems Inc. Bannockburn, USA, for the experiments.

Fluorescence energy transfer experiments onto the live cells

Fluorescence resonance energy transfer (FRET) experiments were performed by utilizing the NBD- and Rho-labeled peptides onto the live mammalian, hRBCs, and 3T3 and bacteria, *E. coli*, *E. coli* ATCC 10536 and *S. aureus* followed by their analyses by flow cytometry as reported (Giddings et al. 2003) earlier with the excitation and emission wavelengths set at 488 and 533 nm, respectively, for NBD. Equimolar amounts of NBD-labeled peptide (donor) and Rho-labeled peptide (acceptor) were added to the hRBCs ($\sim 3 \times 10^7$ cells/ml) or 3T3 ($\sim 10^5$ cells/ml) and *E. coli* or *E. coli* ATCC 10536 or *S. aureus* ($\sim 5 \times 10^5$ CFU/ml) and incubated at 37°C for 10 min (mammalian cells) and 30 min (bacteria), respectively. For FRET experiments fluorescence (X-axis value) of a particular kind of cells in the presence of NBD-labeled peptide (D) and unlabeled peptide (U) was compared to the fluorescence of the cells that was recorded in the presence of NBD-labeled peptide and the corresponding Rho-labeled peptide (A).

Gel electrophoresis

To detect the oligomeric states of the peptides, they were run in SDS-PAGE using 16.5% gel. LZP, SASA and DASA were incubated with hRBCs ghost membrane or 3T3 cells (Tweten et al. 1991) and *E. coli* or *S. aureus* spheroplasts (Papo and Shai 2005) and PC/Chol or PC/PG lipid vesicles for 1 h at 37°C prior to the loading. Rho-labeled peptides were used to determine the oligomeric states of the peptides in the presence of mammalian and bacterial cell membrane in order to avoid background protein bands as reported (Bilgicer and Kumar 2004).

Results

SASA and DASA exhibited lower cytotoxicity against hRBCs and murine 3T3 cells than LZP

To further look into the cytotoxic activity of these peptides against other mammalian cells, viability of the murine fibroblasts 3T3 cells were detected in the presence of these peptides (see the experimental procedure in the supplementary section). MTT assay showed that the viability of 3T3 cells also increased progressively when LZP was replaced by SASA and DASA, respectively (Supplementary Figure 1). Probably, the result points toward the role of the hydrophobic leucine residues at the 'a' and 'd' positions in the leucine zipper sequence in controlling the cytotoxic activity of these peptides against the mammalian cells. Flow cytometric studies to determine the peptide-induced damage of organization of hRBC membrane or the assembly of the peptides onto these cells have been carried out with 3×10^7 cells/ml, which is equivalent to 0.6% (v/v) hRBCs in PBS. Since our previous experiments (Ahmad et al. 2006) were carried out with 6.0% (v/v) hRBCs, hemolytic activity of LZP and its analogs were further checked with 0.6% hRBCs (experimental procedure included in supplementary section). Very similar to our previous results, hemolytic activity of the peptides decreased progressively from LZP to SASA and to DASA (Supplementary Figure 2).

SASA and DASA were much less active in damaging the membrane organization of hRBCs and 3T3 cells as compared to LZP but damaged *E. coli* and *S. aureus* cells equally to LZP

To evaluate the peptide-induced damage of hRBCs or alteration of hRBC membrane phospholipid asymmetry, peptide-treated cells were incubated with FITC labeled annexin V and then analyzed by flow cytometry (Yadav et al. 2008, 2009). Annexin V-FITC does not bind to normal hRBCs since phosphatidyl serine lies in the inner layer of the membrane. However, a treatment of hemolytic protein/peptide (Yadav et al. 2008, 2009) induces a change in organization of hRBC membrane which presumably exposes PS and thus the cells are stained by annexin V-FITC. As shown in Fig. 1a, control hRBCs without any peptide treatment did not show any appreciable staining by annexin V-FITC as expected. However, when the cells were treated with 26.0 μ M of LZP or SASA or DASA a shift of dots of ~ 43 , ~ 15 , and $\sim 4\%$, respectively, to the upper right quadrant (Fig. 1b–d) was observed indicating that the ability of the peptides to damage the membrane organization of hRBC progressively and appreciably reduced from LZP to SASA and to DASA. Highlights of

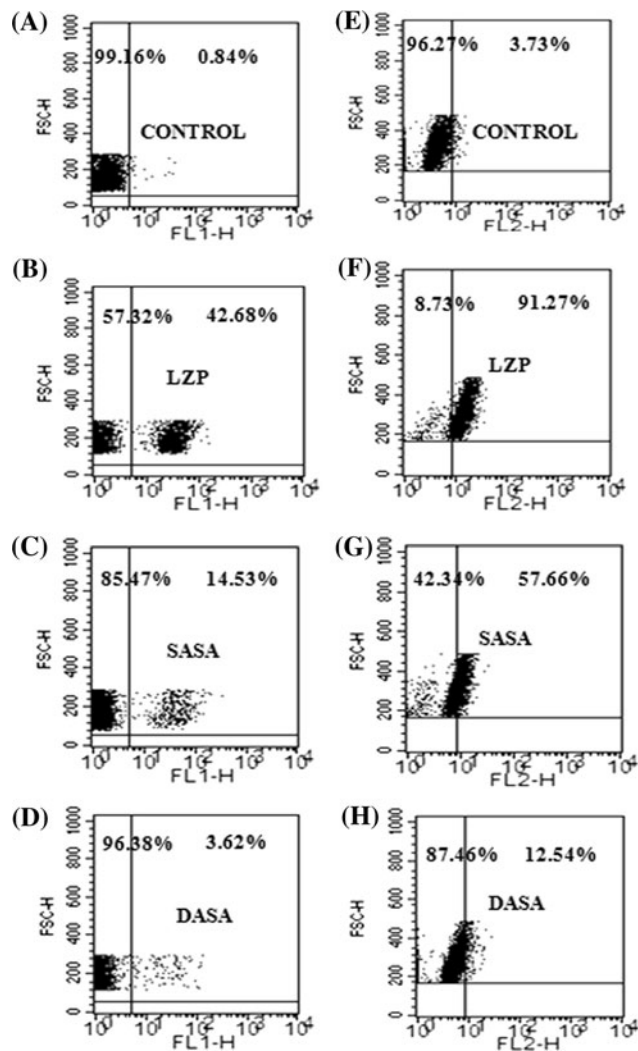


Fig. 1 Detection of peptide-induced perturbation of membrane organization of hRBCs and 3T3 cells by flow cytometric studies. The left (a–d) and right (e–h) hand side, respectively, depict the FITC-annexin V staining of hRBCs and PI staining of 3T3 cells after the treatment with different peptides. a–d the FITC-annexin V staining of hRBCs without any peptide treatment, or treated with 26.0 μ M of LZP, SASA and DASA, respectively. While the panels in the right hand side show the PI staining of 3T3 cells, without any peptide treatment (e) and treated with \sim 12.60 μ M of LZP (f), SASA (g) and DASA (h). On Y axis, FSC-Height is forward scattered height which shows the distribution of the cells. In X axis, FL1-Height means fluorescence recorded by fluorescent filter 1 (green channel) and FL2 means fluorescence recorded by fluorescent filter 2 (red channel). 10,000 events were counted for each experiment

quadrant statistics of data in Fig. 1 have been presented in Supplementary Figure 3.

The effect of LZP and its analogs on murine fibroblasts 3T3 cells, and bacteria, *E. coli* and *S. aureus* was probed by incubating the peptide-treated cells with the DNA intercalating dye propidium iodide (PI). Although PI is impermeable to normal viable cells it can interact with DNA of the cells whose membranes have been damaged, and stain them.

PI staining of 3T3 cells following the treatment of the peptides (\sim 12.6 μ M) showed that LZP damaged these cells to the maximum extent (\sim 91%) followed by SASA (\sim 58%) and DASA (\sim 13%) (Fig. 1f–h, quadrant statistics have been presented in Supplementary Figure 3) as was also observed when the hRBCs were treated with these peptides. Overall, the peptide-induced damage of either hRBC or 3T3 cell membrane showed a similar trend in progressive decrease with substitution of leucine by alanine residues at the ‘a’ and/or ‘d’ position of the heptad repeat of LZP.

However, contrasting results were obtained when either the two strains of *E. coli* or *S. aureus* were stained with PI following the treatment of LZP, SASA and DASA. While the control bacteria treated without any peptide showed no PI fluorescence (Supplementary Figure 4A and E), bacteria treated with \sim 8.0 μ M LZP or SASA or DASA showed an almost similar shift (\sim 80% for *E. coli* and *S. aureus*) of the dots to the upper right quadrant (*E. coli*; Supplementary Figure 4B, C and D and *S. aureus*; Supplementary Figure 4 F, G and H; highlights of quadrant statistics have been shown in Supplementary Figure 5) indicating a similar and appreciable staining of both the bacteria by PI following the treatment of either LZP or its alanine-substituted analogs SASA and DASA. Furthermore, *E. coli* ATCC 10536 cells were almost very similarly stained by PI following the treatment of any of these three peptides (Supplementary Figure 6). The data showed that unlike their unequal ability to damage the organization of hRBC or 3T3 cell membrane, all three peptides caused a comparable damage to bacterial cell membrane organization.

Moreover, the ability of NBD-labeled peptides to damage the membrane organization of *S. aureus* was determined by PI staining of the cells to investigate whether the labeling of peptides disturbs their functional activity or not. The dot plots (Supplementary Figure 7) showed that bacteria bound to NBD-labeled peptides were also stained by PI. The result indicated that NBD-labeled peptides damaged bacterial membranes and therefore PI stained the bacteria. Similar amounts of NBD-labeled LZP or SASA or DASA caused to some extent higher (\sim 10%) PI staining of bacteria as compared to their unlabeled counterparts (Supplementary Figure 7). The data suggest that probably NBD-labeling resulted in a minor increase in interaction of these three peptides with *S. aureus*. (experimental procedure has been included in supplementary material section).

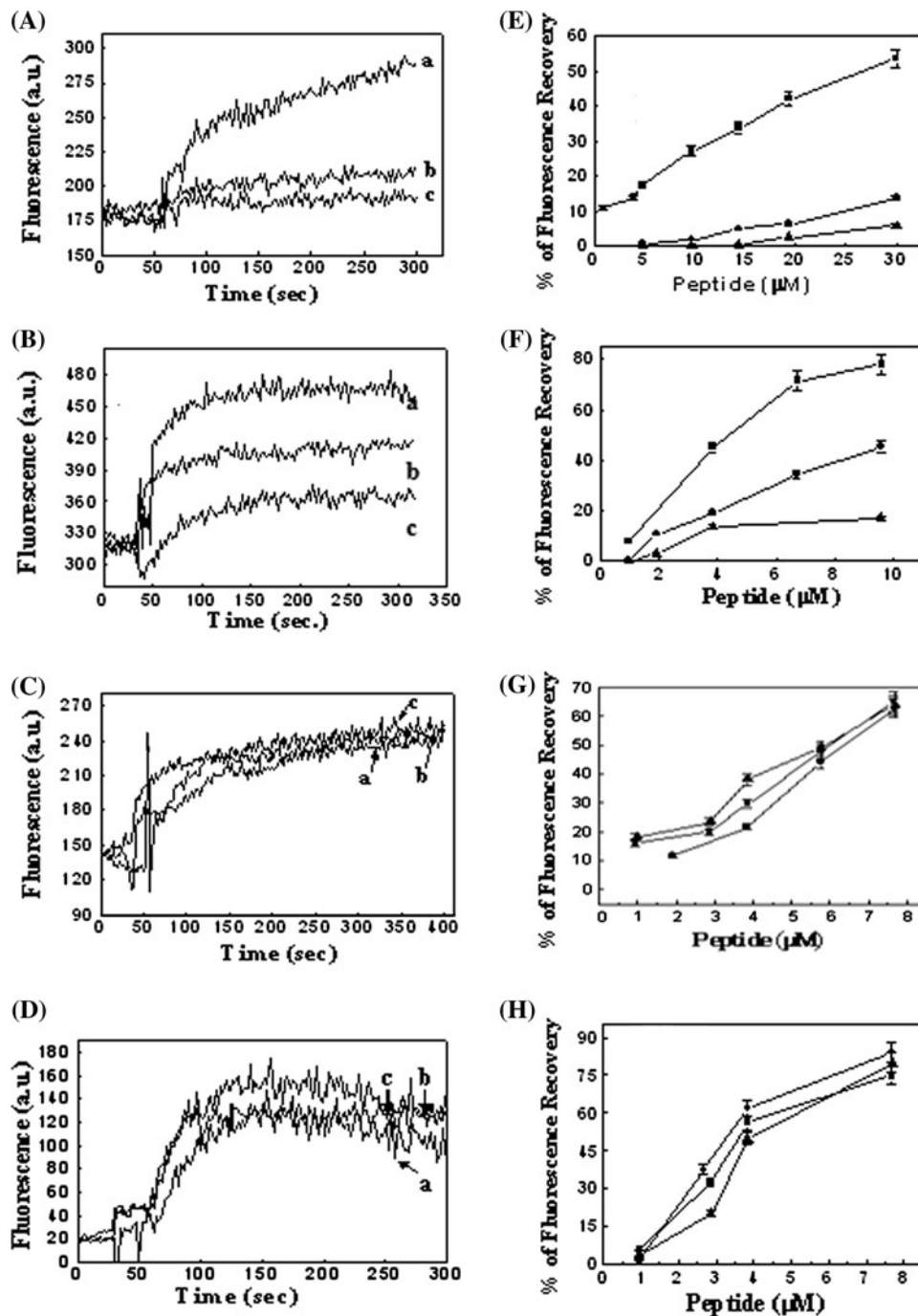
Significant differences between LZP and its analogs in depolarizing the hRBC and 3T3 cell membrane though the peptides depolarized *E. coli* and *S. aureus* membrane to a similar extent

To understand the mode of action of these peptides, their efficacy to induce permeation in mammalian and bacterial

cell membranes was determined by measuring the peptide-induced membrane depolarization of hRBC, 3T3, *E. coli* and *S. aureus* cells. As evidenced from the peptide-induced fluorescence recovery data, which is a measure of peptide-induced cell membrane permeation, LZIP showed the highest efficacy to induce permeation in hRBC as well as 3T3 cell membranes (Fig. 2A, B, E, F). However, LZIP-induced permeability of hRBC and 3T3 cell membranes significantly and progressively decreased when this peptide

was replaced by SASA and DASA, respectively (Fig. 2E, F). Contrastingly, LZIP, SASA and DASA induced very similar fluorescence recovery in *E. coli* as well as *S. aureus* cells indicating that all three peptides permeabilized these bacterial cell membranes (Fig. 2C, D, G, H) with similar efficacy. Membrane depolarization of *S. aureus* and hRBCs was also measured in the presence of fluorescently-labeled LZIP, SASA and DASA to detect the effect of labeling these peptides by fluorescent probes on their membrane

Fig. 2 Dose-dependent peptide-induced transmembrane depolarization of mammalian, hRBC and murine 3T3 cells and bacteria namely *E. coli* and *S. aureus*. **A, B** the representative profiles of membrane depolarization of hRBC (peptide concentration $\sim 30.0 \mu\text{M}$) and 3T3 (peptide concentration $\sim 9.6 \mu\text{M}$) cells induced by either LZIP (**a**) or SASA (**b**) or DASA (**c**). **C, D** the representative profiles of membrane depolarization of *E. coli* and *S. aureus* induced by $\sim 8.0 \mu\text{M}$ of LZIP (**a**), SASA (**b**) and DASA (**c**). **E–H** show the plot of the percentage of fluorescence recovery, which is a measure of transmembrane depolarization, versus peptide concentration in μM of hRBC, 3T3, *E. coli* and *S. aureus* cells, respectively. **solid square** LZIP, **solid circle** SASA, **solid triangle** DASA



permeabilizing properties toward these cells. It was observed that NBD- and Rho-labeled LZIP, SASA and DASA induced very similar membrane depolarization as their unlabeled versions in hRBCs and *S. aureus* (Supplementary Figure 8), respectively, indicating that the labeling of these peptides did not alter their membrane permeabilizing properties significantly.

SASA and DASA exhibited weaker assembly as compared to LZIP onto mammalian cells but showed comparable assembly to LZIP onto the bacteria

To understand a plausible role of cellular assembly of LZIP and its analogs in determining their cytotoxic and antibacterial activities, FRET experiments were performed onto the live mammalian, hRBC and 3T3 cells and bacteria, *E. coli*, *E. coli* ATCC 10536 and *S. aureus* with their NBD- and Rho-labeled versions and analyzed by flow cytometry. Equimolar amounts of NBD-labeled peptides (donor) and either unlabeled peptides or Rho-labeled peptides (acceptor) were incubated with hRBCs or 3T3 cells. Changes in the fluorescence of hRBC or 3T3 cells in the presence of donor peptide were compared when the acceptor-labeled peptides were replaced by the corresponding unlabeled peptides. The fluorescence intensity (the X-axis value) of hRBC or 3T3 cells in the presence of NBD-LZIP decreased appreciably when unlabeled LZIP was replaced by Rho-LZIP indicating energy transfer events which result from the self-association of the NBD- and Rho- labeled peptide molecules onto the live hRBCs (Fig. 3a) or 3T3 cells (Fig. 3d). However, when the same experiments were performed with NBD- and Rho-labeled SASA, the extent of energy transfer was lesser indicating to some extent weaker assembly among the SASA peptide molecules onto the live hRBCs (3b) or 3T3 cells (Fig. 3e) than the LZIP molecules. For DASA the extent of energy transfer further decreased significantly onto both the live cells (Fig. 3c for hRBCs; Fig. 3f for 3T3 cells) as evidenced by the insignificant decrease in NBD-DASA fluorescence (the negligible shift of fluorescence peak on the X-axis toward left hand side) after the addition of Rho-DASA peptide suggesting that the DASA peptide molecules assembled most weakly among the three peptides onto either hRBCs or murine 3T3 cells. The results clearly indicated that the extent of energy transfer onto hRBCs and 3T3 cells decreased from LZIP to SASA and to DASA.

Interestingly, when FRET experiments were performed onto the live *E. coli* (Fig. 4a–c), *E. coli* ATCC 10536 (Supplementary Figure 6) and *S. aureus* (Fig. 4d–f) cells in a similar way, for all three peptides, the NBD-fluorescence of the bacteria decreased appreciably when the respective unlabeled peptide was replaced by the

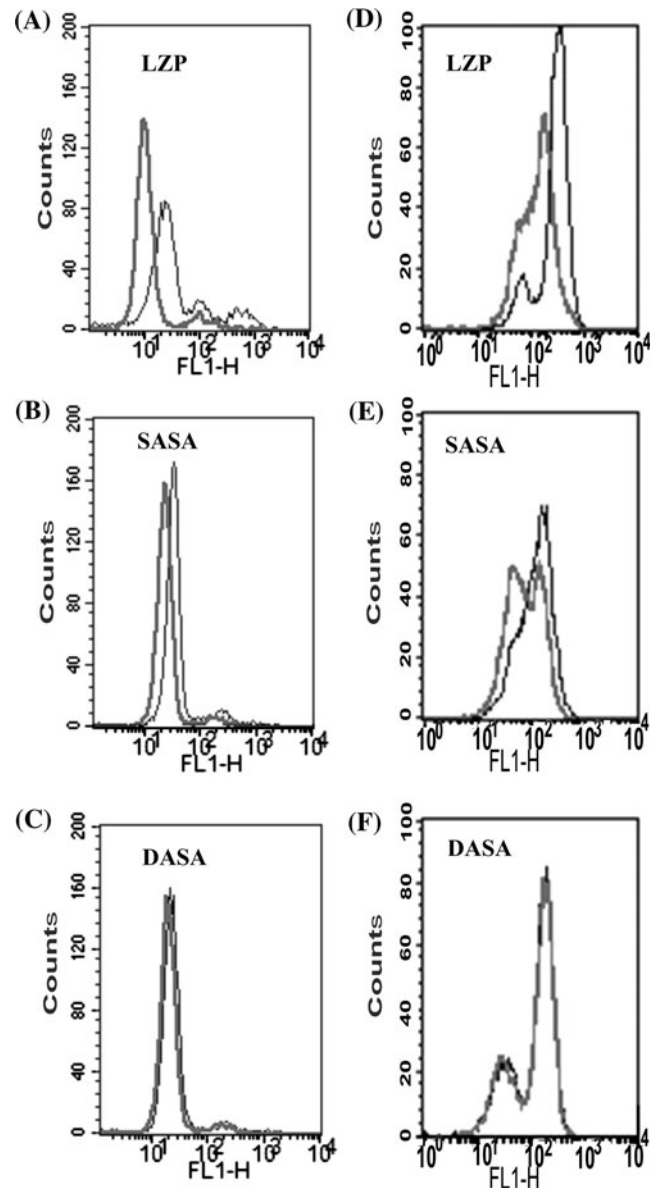


Fig. 3 Detection of self-assembly of the LZIP, SASA and DASA onto the live hRBCs (left hand side) and 3T3 cells (right hand side) by FRET experiments with the help of flow cytometry. Equimolar amounts of donor- (NBD) labeled peptides (D) and either the corresponding unlabeled peptide (U) or acceptor- (Rho) labeled peptide (A) incubated with hRBCs (a–c) or 3T3 cells (d–f) at 37°C and then analyzed by flow cytometry. Black (thinner) and gray (thicker) lines represent (D + U) and (D + A), respectively. a–c show the FRET experiments onto hRBCs with LZIP, SASA and DASA, respectively, with ~10.0 µM of each of the peptides while d–f show the FRET experiments onto 3T3 cells with LZIP, SASA and DASA, respectively, for a peptide concentration of ~5.7 µM for each of them. 10,000 events were counted for each sample

corresponding Rho-labeled peptide. The data clearly indicated appreciable energy transfer between the NBD- and Rho-labeled versions for all the three peptides which resulted from their self-association onto the two *E. coli* strains and *S. aureus*.

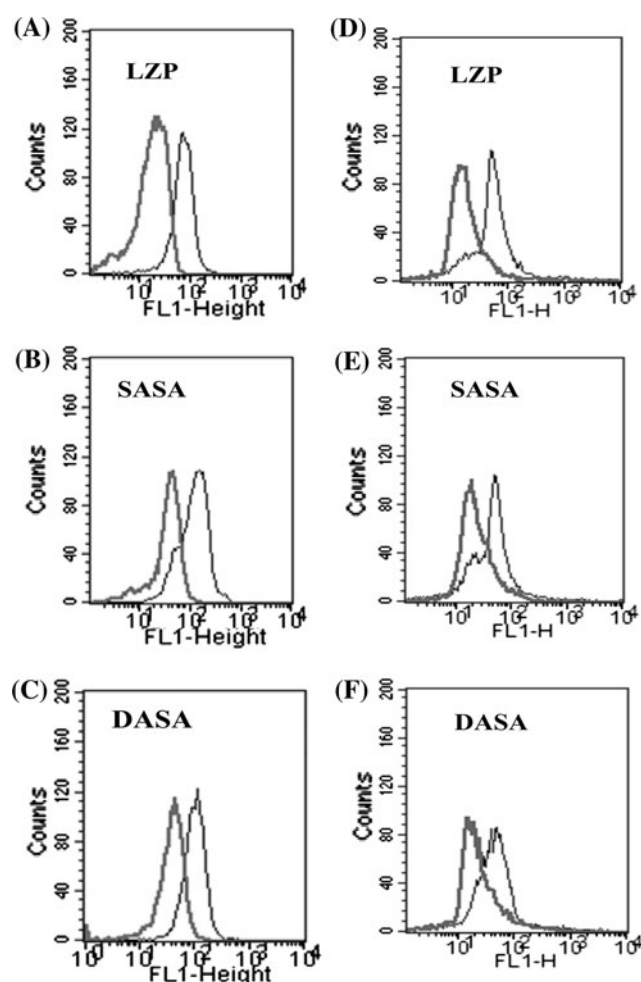


Fig. 4 Detection of self-assembly of the LZIP, SASA and DASA onto live *E. coli* (left hand side) and *S. aureus* cells (right hand side) by FRET experiments with the help of flow cytometry. Equimolar amounts of donor- (NBD) labeled peptides (D) and either the corresponding unlabeled peptide (U) or acceptor- (Rho) labeled peptide (A) incubated with *E. coli* (a–c) or *S. aureus* cells (d–f) at 37°C and then analyzed by flow cytometry. Black (thinner) and gray (thicker) lines represent (D + U) and (D + A), respectively. a–c show the FRET experiments onto *E. coli* with LZIP, SASA and DASA, respectively, with $\sim 8 \mu\text{M}$ of each of the peptides while d–f show the FRET experiments onto *S. aureus* cells with LZIP, SASA and DASA, respectively, for a peptide concentration of $\sim 7.2 \mu\text{M}$ for each of them. 10,000 events were counted for each experiment

SASA and DASA exhibited lower oligomeric states as compared to LZIP only in mammalian cell membrane or in zwitterionic lipid vesicle but not in bacterial membrane or in negatively charged lipid vesicles

To further determine the oligomeric states of LZIP, SASA and DASA in the presence of these mammalian and bacterial cell membranes and understand its role in the cytotoxic and bactericidal activities of the peptides, SDS–PAGE experiments were performed with these peptides in the presence of hRBCs ghost membrane and 3T3

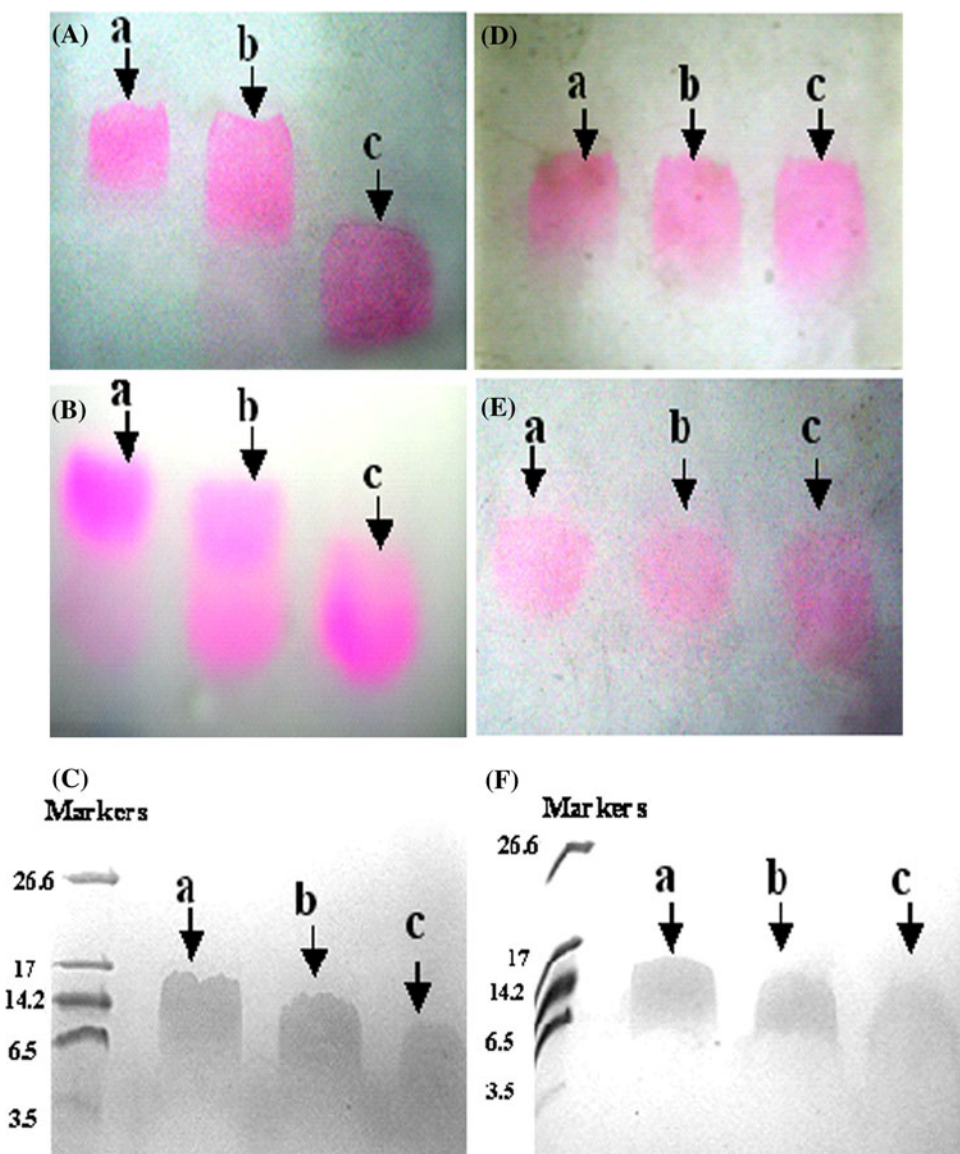
membrane and *E. coli* and *S. aureus* spheroplasts. Furthermore, oligomeric states of LZIP, SASA and DASA were also examined by SDS–PAGE experiments in the presence of both kinds of model membranes namely zwitterionic, PC/Chol and negatively charged, PC/PG lipid vesicles. While comparing the oligomeric states of LZIP and its analogs in the presence of mammalian and bacterial cell membranes, Rho-labeled versions of the peptides were used and the gels were not stained by coomassie blue to avoid the background protein bands of these cell membranes (Bilgicer and Kumar 2004). Therefore, the regular molecular weight markers are missing in the representation of these gel pictures (Fig. 5A, B, D, E). LZIP formed significant oligomeric structure in both PC/Chol lipid vesicles (lane a, Fig. 5C) or in hRBCs ghost membrane (lane a, Fig. 5A) and 3T3 (lane a, Fig. 5B) cell membrane while the SASA formed slightly lesser oligomeric structure (lane b, Fig. 5A–C) and DASA exhibited the least oligomeric states (lane c, Fig. 5A–C) in all three environments.

In contrast, LZIP, SASA and DASA adopted considerable and comparable oligomeric states either in bacterial spheroplasts or in the presence of PC/PG lipid vesicle (lanes a–c, Fig. 5D–F) suggesting that all three peptides exhibited comparable oligomeric assembly in the presence of either negatively charged lipid vesicles and/or *E. coli* and *S. aureus* cell membrane.

Discussion

There are several reports in the literature that the substitution of leucine by alanine at the ‘a’/‘d’ position of leucine zipper sequence in a protein significantly impair its oligomeric state which often results in the loss of its functional activity (Luo et al. 1999; Nagoshi and Yoneda 2001; Richie-Jannetta et al. 2003). In our previous study it has been shown that substitution of leucine by alanine at the ‘a’/‘d’ position of leucine zipper sequence significantly and progressively reduced the lytic activity of the LZIP peptide against hRBCs (Ahmad et al. 2006). Moreover, CD, gel filtration studies, and tryptophan fluorescence experiments clearly indicated that LZIP was more self-associated or oligomerized as compared to its analogs in aqueous environment (Ahmad et al. 2006). However, it is not known from the previous study, how these peptides self-assemble onto hRBCs and bacteria or lipid vesicles and its influence on their antibacterial and cytotoxic activities. Therefore, in the present investigation we have studied the self-assembly or oligomeric states of LZIP, SASA and DASA onto the representative live mammalian cells and bacteria and in the presence of these cell membranes and lipid vesicles that mimic these cell membranes to understand the influence of leucine to alanine substitution in the assembly of LZIP in

Fig. 5 Detection of oligomeric states of the peptides in the presence of hRBC ghost membrane (A), 3T3 cells (B) and PC/Chol lipid vesicles (C), *E. coli* spheroplasts (D), *S. aureus* spheroplasts (E) and PC/PG lipid vesicles (F). In all three panels, lanes *a*, *b* and *c* show the LZP, SASA and DASA, respectively. For C, F 15 μ g of each of the peptides were loaded whereas for A, B, D, E 12 μ g of each of the Rho-labeled peptides were loaded



different environments and its possible role in determining the cytotoxic and antibacterial activity of these peptides. Furthermore, permeabilization and destabilization of organization of different cell membranes in the presence of these peptides was studied in order to comprehend the effect of any alteration in the assembly of these peptides onto their functional activities. To our knowledge, the present work for the first time reports the study on the assembly of membrane-active antimicrobial peptides onto both live mammalian cells and bacteria as well as in the presence of these cell membranes and corresponding model membranes with respect to their ability to permeabilize or damage the organization of these cellular membranes.

The progressive decrease in peptide-induced damage of membrane organization (Fig. 1) and permeability (Fig. 2E, F) of hRBC and 3T3 cell membranes by LZP, SASA and

DASA matched well with the decrease in their hemolytic activities against the hRBCs (Ahmad et al. 2006) (Supplementary Figure 2) and the increase in viability of 3T3 cells in the presence of the peptides (Supplementary Figure 1) in the same order. Moreover, our confocal microscopic studies (Ahmad et al. 2006) with NBD-labeled peptides showed stronger binding and distinct localization of LZP to hRBCs as compared to its analogs. On the other hand, similar membrane permeabilizing/membrane-damaging activity of LZP, SASA and DASA toward *E. coli* or *S. aureus* cells (Figs. 2G, H; 3) was consistent with their comparable antibacterial activities against the bacteria (Ahmad et al. 2006).

CD experiments showed that only LZP but not its alanine-substituted analogs SASA and DASA adopted significant helical structure in PBS (Ahmad et al. 2006)

despite the slightly better helix propensity of alanine than leucine in aqueous environment (Liu and Deber 1998). LZP maintains its helical structure in the presence of zwitterionic and negatively charged lipid vesicles. Though leucine has only slightly higher helix propensity than alanine in non-polar environment (Liu and Deber 1998), SASA and DASA showed drastically reduced helicity in the presence of zwitterionic lipid vesicles as compared to that of LZP. However, SASA and DASA adopted appreciable and very similar helical structures as LZP in the presence of negatively charged lipid vesicles (Ahmad et al. 2006). It is noteworthy that the contrasting secondary structures of these peptides in the presence of negatively charged and zwitterionic lipid vesicles match well with their distinct self-association properties in the respective environment (Fig. 5).

Fluorescence energy transfer and gel electrophoresis experiments indicated that assembly and oligomeric states of LZP onto live hRBCs or 3T3 cells and in the presence of these cell membranes decreased progressively following the substitution of leucine by alanine residue (s) at 'a' and/or 'd' position (s) of its heptad repeat (Figs. 3, 5). LZP showed the strongest assembly among the three peptides onto live hRBCs and 3T3 cells or the highest oligomeric states in the presence of these cell membranes, which probably assisted these molecules to permeabilize these cell membranes appreciably and exhibit the highest cytotoxic activity against these cells. Cytotoxic Temporin L, Protegrin-1 and LL-37 were reported to self-assemble in the presence of mammalian cell membrane mimetic zwitterionic lipid vesicles (Oren et al. 1999; Mahalka and Kinnunen 2009; Mani et al. 2006). On the other hand, the single and double alanine substituted analogs of LZP exhibited progressively weaker assembly onto these live mammalian cells (Fig. 3) or gradually lower oligomeric states in the presence of these cell membranes (Fig. 5), which could be related to the progressive decrease in the peptide-induced permeabilization of these cells and thus the SASA and DASA showed lower and the lowest cytotoxicity, respectively, among the three peptides against the tested mammalian cells.

In contrast, LZP, SASA and DASA appreciably self-assembled onto live *E. coli* strains and *S. aureus* (Fig. 4). Moreover, all three peptides exhibited comparable oligomeric states in the presence of *E. coli* or *S. aureus* spheroplasts (Fig. 5). Probably, the comparable self-assembly/oligomeric states of LZP, SASA and DASA onto these bacterial membrane may assist in maintaining their similar activity in permeabilizing/damaging the bacterial membrane which could be further associated with their comparable antibacterial activities against these bacteria. The aggregation properties of different Temporins, Protegrin-1, and designed peptides in the presence of negatively

charged lipid vesicles have been studied (Glukhov et al. 2005; Mahalka and Kinnunen 2009; Mani et al. 2006). Contrasting self-assembly of BMAP-28 and BMAP-27 and their non-toxic analogs onto mammalian live cells have been reported (Ahmad et al. 2009a, b) recently. Interestingly, both of these wild type peptides as well as their selected analogs showed comparable antibacterial activity and also self-assembled appreciably onto live bacteria (Ahmad et al. 2009a, b).

The oligomeric states of these peptides were also determined in the presence of zwitterionic PC/Chol and negatively charged PC/PG lipid vesicles lipid vesicles which are often used as model membrane mimetic of mammalian and bacterial cells (Hawrani et al. 2008; Pan et al. 2007; Zhang et al. 2001), respectively. As shown in Fig. 5 very similar to the oligomeric properties of these Rho-labeled peptides in the presence of hRBC ghost membrane or 3T3 cell membrane, oligomeric states of the unlabeled peptides progressively decreased from LZP to SASA and to DASA in the zwitterionic PC/Chol lipid vesicles. In contrast, all three peptides showed an almost similar oligomeric states in the negatively charged lipid vesicles and in the presence of *E. coli* or *S. aureus* cell membrane (Fig. 5). These results probably indicate that the lipids present in the membrane of mammalian and bacterial cells including the different nature of their electrical charge could contribute significantly in the differences between LZP and its analogs in their assembly and oligomeric states in the tested mammalian and bacterial cell membranes. It is to be mentioned that despite these studies, membrane interaction of these peptides are not very clear on a molecular level and need further research to evaluate it.

In summary, the results presented here show an appreciable correlation between the assembly of LZP, SASA and DASA onto the tested live mammalian cells and bacteria or in the presence of these cell membranes and mimetic lipid vesicles with respect to their cytotoxic and bactericidal activities against the respective cells. The results showed a probable role of leucine zipper sequence in the self-assembly/oligomeric state of LZP and its analogs in different membrane environments studied here. Despite detailed studies from the current findings it is difficult to understand the mechanism of peptide-membrane interaction or self-assembly of these peptides in different membrane environments. However, the present study may help in understanding the cytotoxicity and antibacterial activities of LZP and its analogs and also in designing the membrane-active, cell-selective peptides by altering their assembly in a particular cell membrane.

Acknowledgments The work was supported by the CSIR network project NWP 0005. The authors are extremely thankful to A. L. Vishwakarma for recoding the flow cytometry profiles. Brijesh Kumar

Pandey is acknowledged for his contribution in preparation of revised version of the manuscript. A. A and S.A. acknowledge the receipt of a senior and junior research fellowship from CSIR, India, respectively.

References

- Ahmad A, Yadav SP, Asthana N, Mitra K, Srivastava SP, Ghosh JK (2006) Utilization of an amphipathic leucine zipper sequence to design antibacterial peptides with simultaneous modulation of toxic activity against human red blood cells. *J Biol Chem* 281:22029–22038
- Ahmad A, Asthana N, Azmi S, Srivastava RM, Pandey BK, Yadav V, Ghosh JK (2009a) Structure-function study of cathelicidin-derived bovine antimicrobial peptide BMAP-28: design of its cell-selective analogs by amino acid substitutions in the heptad repeat sequences. *Biochim Biophys Acta* 1788:2411–2420
- Ahmad A, Azmi S, Srivastava RM, Srivastava S, Pandey BK, Saxena R, Bajpai VK, Ghosh JK (2009b) Design of nontoxic analogues of cathelicidin-derived bovine antimicrobial peptide BMAP-27: the role of leucine as well as phenylalanine zipper sequences in determining its toxicity. *Biochemistry* 48:10905–10917
- Asthana N, Yadav SP, Ghosh JK (2004) Dissection of antibacterial and toxic activity of melittin: a leucine zipper motif plays a crucial role in determining its hemolytic activity but not antibacterial activity. *J Biol Chem* 279:55042–55050
- Bilgicer B, Kumar K (2004) De novo design of defined helical bundles in membrane environments. *Proc Natl Acad Sci USA* 101:15324–15329
- Boman HG (1995) Peptide antibiotics and their role in innate immunity. *Annu Rev Immunol* 13:61–92
- Chen Y, Mant CT, Farmer SW, Hancock RE, Vasil ML, Hodges RS (2005) Rational design of alpha-helical antimicrobial peptides with enhanced activities and specificity/therapeutic index. *J Biol Chem* 280:12316–12329
- Ghosh JK, Shaool D, Guillaud P, Ciceron L, Mazier D, Kustanovich I, Shai Y, Mor A (1997) Selective cytotoxicity of dermaseptin S3 toward intraerythrocytic *Plasmodium falciparum* and the underlying molecular basis. *J Biol Chem* 272:31609–31616
- Giddings KS, Johnson AE, Tweten RK (2003) Redefining cholesterol's role in the mechanism of the cholesterol-dependent cytolysins. *Proc Natl Acad Sci USA* 100:11315–11320
- Glukhov E, Stark M, Burrows LL, Deber CM (2005) Basis for selectivity of cationic antimicrobial peptides for bacterial versus mammalian membranes. *J Biol Chem* 280:33960–33967
- Hancock RE (1997) Peptide antibiotics. *Lancet* 349:418–422
- Hancock RE, Sahl HG (2006) Antimicrobial and host-defense peptides as new anti-infective therapeutic strategies. *Nat Biotechnol* 24:1551–1557
- Hawrani A, Howe RA, Walsh TR, Dempsey CE (2008) Origin of low mammalian cell toxicity in a class of highly active antimicrobial amphipathic helical peptides. *J Biol Chem* 283:18636–18645
- Hilpert K, Volkmer-Engert R, Walter T, Hancock RE (2005) High-throughput generation of small antibacterial peptides with improved activity. *Nat Biotechnol* 23:1008–1012
- Javadpour MM, Barkley MD (1997) Self-assembly of designed antimicrobial peptides in solution and micelles. *Biochemistry* 36:9540–9549
- Lai Y, Gallo RL (2009) AMPed up immunity: how antimicrobial peptides have multiple roles in immune defense. *Trends Immunol* 30:131–141
- Li WF, Ma GX, Zhou XX (2006) Apidaecin-type peptides: biodiversity, structure–function relationships and mode of action. *Peptides* 27:2350–2359
- Liu LP, Deber CM (1998) Uncoupling hydrophobicity and helicity in transmembrane segments. Alpha-helical propensities of the amino acids in non-polar environments. *J Biol Chem* 273:23645–23648
- Luo Z, Matthews AM, Weiss SR (1999) Amino acid substitutions within the leucine zipper domain of the murine coronavirus spike protein cause defects in oligomerization and the ability to induce cell-to-cell fusion. *J Virol* 73:8152–8159
- Luque-Ortega JR, van't Hof W, Veerman EC, Saugar JM, Rivas L (2008) Human antimicrobial peptide histatin 5 is a cell-penetrating peptide targeting mitochondrial ATP synthesis in *Leishmania*. *FASEB J* 22:1817–1828
- Mahalka AK, Kinnunen PK (2009) Binding of amphipathic alpha-helical antimicrobial peptides to lipid membranes: lessons from temporins B and L. *Biochim Biophys Acta* 1788:1600–1609
- Mani R, Cady SD, Tang M, Waring AJ, Lehrer RI, Hong M (2006) Membrane-dependent oligomeric structure and pore formation of a beta-hairpin antimicrobial peptide in lipid bilayers from solid-state NMR. *Proc Natl Acad Sci USA* 103:16242–16247
- Marr AK, Gooderham WJ, Hancock RE (2006) Antibacterial peptides for therapeutic use: obstacles and realistic outlook. *Curr Opin Pharmacol* 6:468–472
- Nagoshi E, Yoneda Y (2001) Dimerization of sterol regulatory element-binding protein 2 via the helix-loop-helix-leucine zipper domain is a prerequisite for its nuclear localization mediated by importin beta. *Mol Cell Biol* 21:2779–2789
- Nicolas P (2009) Multifunctional host defense peptides: intracellular-targeting antimicrobial peptides. *FEBS J* 276:6483–6496
- Oren Z, Shai Y (1997) Selective lysis of bacteria but not mammalian cells by diastereomers of melittin: structure-function study. *Biochemistry* 36:1826–1835
- Oren Z, Lerman JC, Gudmundsson GH, Agerberth B, Shai Y (1999) Structure and organization of the human antimicrobial peptide LL-37 in phospholipid membranes: relevance to the molecular basis for its non-cell-selective activity. *Biochem J* 341(Pt 3):501–513
- Otvos L Jr, Wade JD, Lin F, Condie BA, Hanrieder J, Hoffmann R (2005) Designer antibacterial peptides kill fluoroquinolone-resistant clinical isolates. *J Med Chem* 48:5349–5359
- Pan YL, Cheng JT, Hale J, Pan J, Hancock RE, Straus SK (2007) Characterization of the structure and membrane interaction of the antimicrobial peptides aurein 2.2 and 2.3 from Australian southern bell frogs. *Biophys J* 92:2854–2864
- Papo N, Shai Y (2005) A molecular mechanism for lipopolysaccharide protection of Gram-negative bacteria from antimicrobial peptides. *J Biol Chem* 280:10378–10387
- Patrzykat A, Friedrich CL, Zhang L, Mendoza V, Hancock RE (2002) Sublethal concentrations of pleurocidin-derived antimicrobial peptides inhibit macromolecular synthesis in *Escherichia coli*. *Antimicrob Agents Chemother* 46:605–614
- Podda E, Benincasa M, Pacor S, Micali F, Mattiuzzo M, Gennaro R, Scocchi M (2006) Dual mode of action of Bac7, a proline-rich antibacterial peptide. *Biochim Biophys Acta* 1760:1732–1740
- Richie-Jannetta R, Francis SH, Corbin JD (2003) Dimerization of cGMP-dependent protein kinase I β is mediated by an extensive amino-terminal leucine zipper motif, and dimerization modulates enzyme function. *J Biol Chem* 278:50070–50079
- Tweten RK, Harris RW, Sims PJ (1991) Isolation of a tryptic fragment from *Clostridium perfringens* theta-toxin that contains sites for membrane binding and self-aggregation. *J Biol Chem* 266:12449–12454
- Yadav SP, Kundu B, Ghosh JK (2003) Identification and characterization of an amphipathic leucine zipper-like motif in *Escherichia coli* toxin hemolysin E. Plausible role in the assembly and membrane destabilization. *J Biol Chem* 278:51023–51034

- Yadav SP, Ahmad A, Pandey BK, Verma R, Ghosh JK (2008) Inhibition of lytic activity of *Escherichia coli* toxin hemolysin E against human red blood cells by a leucine zipper peptide and understanding the underlying mechanism. *Biochemistry* 47:2134–2142
- Yadav SP, Ahmad A, Pandey BK, Singh D, Asthana N, Verma R, Tripathi RK, Ghosh JK (2009) A peptide derived from the putative transmembrane domain in the tail region of *E. coli* toxin hemolysin E assembles in phospholipid membrane and exhibits lytic activity to human red blood cells: plausible implications in the toxic activity of the protein. *Biochim Biophys Acta* 1788:538–550
- Yeaman MR, Yount NY (2007) Unifying themes in host defence effector polypeptides. *Nat Rev Microbiol* 5:727–740
- Zasloff M (2002) Antimicrobial peptides of multicellular organisms. *Nature* 415:389–395
- Zasloff M (2006) Inducing endogenous antimicrobial peptides to battle infections. *Proc Natl Acad Sci USA* 103:8913–8914
- Zhang L, Rozek A, Hancock RE (2001) Interaction of cationic antimicrobial peptides with model membranes. *J Biol Chem* 276:35714–35722